

# A USRP-based Testbed for OFDM-based Radar and Communication Systems

Martin Braun, Marcus Müller, Manuel Fuhr, and Friedrich K. Jondral  
Communications Engineering Lab, Karlsruhe Institute of Technology (KIT), Germany  
Kaiserstr. 12  
D-76133 Karlsruhe, Germany  
Email: martin.braun@kit.edu  
Phone: +49 721 608 43790

**Index Terms**—OFDM Radar, Software Defined Radio, USRP

**Abstract**—In this paper, we present a measurement testbed for OFDM radar which uses USRPs as a front-end. The resulting system, using two USRPs and a laptop, requires little power and can thus be easily installed in vehicles to perform measurements for car-to-car or car-to-infrastructure applications. As an example, we show how signals parametrized according to the IEEE 802.11a/p standards can be enhanced by radar functions without any additional spectrum usage and only a little extra signal processing.

## I. INTRODUCTION

Over the last two years, OFDM has become a focus of research for use in mobile networks which combine *radar* and *communications* in a single system [1], [2]. Such systems use information-bearing OFDM signals as radar signals, which allows both a communication usage (other systems can receive and decode this signal) as well as radar functionality (by receiving reflections of the own transmitted signal) with a single access to the medium. Combined radar and communication systems thus save spectrum usage, and any OFDM transmitter can be upgraded with radar features simply by adding a receiver and some digital signal processing. If a receiver chain is already present, the additional hardware requirements are further alleviated.

In our previous publications, the application we have focussed on most was vehicular systems. Both radar and communication systems are becoming more important in future concepts for traffic safety. Some systems are already available, such as radar-aided adaptive cruise control systems or lane-change assistants; others, such as car-to-car communications, are still subject of research but are expected to be integrated into commercially available vehicles in the near future.

Using a technique – such as OFDM radar – which combines both functions has several advantages. From a technical point of view, it enables synergy effects between the systems, e.g. by allowing the radar system to communicate with other participants in the network and thus creating a cooperative radar system. An economical advantage is that a fusion of the two sub-systems makes it worth deploying communication components for vehicles even if the density of participating vehicles is too small to justify a communication-only device.

In previous publications, we have shown through simulations and measurements [3] that OFDM radar systems work both theoretically and practically. However, what is lacking is a simple, small, portable and easily modifiable testbed.

In this paper, we present a software radio-based approach using Universal Software Radio Peripherals (USRPs), which was first described in [4]. Although this hardware is not optimized for radar applications, we can still show that the principle works well.

This paper is structured as follows: in the following section, we will explain the basics of an OFDM radar system and go into some details about the waveforms used. Sections III and IV will describe the measurement setup and show some results, respectively. Finally, section V concludes.

## II. OFDM RADAR BASICS

Like any other radar system, OFDM radar works by transmitting a signal and receiving reflections of this signal from objects in the path of the signal's wavefront. The big difference is that the signal transmitted was not designed for radar purposes (such as an FMCW signal) but to convey information. To then achieve radar imaging requires some signal processing, the basics of which are described very briefly in this section. For a more detailed explanation of the algorithm we refer to previous publications, e.g. [2], [5].

OFDM radar performs one measurement per *frame*, which describes a set of  $M$  consecutive OFDM symbols. Every OFDM symbol uses  $N$  active carriers to transmit (e.g. for OFDM signals following the IEEE 802.11a/p standard,  $N$  would be 53 including an empty DC carrier). As in previous publications, we denote a transmitted OFDM frame by a matrix,

$$\mathbf{F}_{\text{Tx}} = \begin{pmatrix} c_{0,0} & \cdots & c_{0,M-1} \\ c_{1,0} & \cdots & c_{1,M-1} \\ \vdots & \ddots & \vdots \\ c_{N-1,0} & \cdots & c_{N-1,M-1} \end{pmatrix}. \quad (1)$$

In plain language, every row of the matrix corresponds to the data on one sub-carrier, whereas every column corresponds to the data on one OFDM symbol. One element  $c_{k,l}$  from this matrix is a complex value from a modulation alphabet, most

often BPSK or QPSK. A transmit matrix can be converted into a *transmit signal* simply by

- applying an IFFT of length  $N_{\text{Total}}$  on every column,
- adding a cyclic prefix and
- digital/analog converting it.

This matrix is therefore equivalent to the actual signal transmitted if the following parameters are known:

- The sub-carrier distance  $\Delta f$ , and therefore the OFDM symbol duration  $T = 1/\Delta f$ .
- The duration of the cyclic prefix (or guard interval),  $T_G$ .
- The sampling rate  $f_S$  after the IFFT. Note that this determines the sub-carrier distance by  $\Delta f = \frac{f_S}{N_{\text{Total}}}$ .
- The centre frequency  $f_C$ .

While transmitting, a receiver is active to pick up backscattered signals. It is important that the receiver is exactly synchronous to the transmitter, meaning that there must be no time or frequency offset. If these conditions are met, a received signal can also be represented by a matrix,

$$(\mathbf{F}_{\text{Rx}})_{k,l} = \sum_{h=0}^{H-1} b_h (\mathbf{F}_{\text{Tx}})_{k,l} \cdot e^{j2\pi T_O f_{D,h} l} \cdot e^{-j2\pi \tau_h \Delta f k} \cdot e^{j\varphi_h} + (\tilde{\mathbf{Z}})_{k,l}. \quad (2)$$

Here,  $H$  denotes the number of reflecting targets. Every target has a distance  $d_h$ , which translates into a delay  $\tau_h$  of the corresponding signal.  $f_{D,h}$  is its Doppler shift, and  $\varphi_h$  is a random, unknown phase shift. The attenuation  $b_h$  for each target can be approximated by the point-scatterer model [6],

$$b_h = \sqrt{\frac{c_0 \sigma_{\text{RCS},h}}{(4\pi)^3 d_h^4 f_C^2}}, \quad (3)$$

where  $\sigma_{\text{RCS},h}$  is the radar cross section. The matrix  $\mathbf{Z} \in \mathbb{C}^{N \times M}$  represents white Gaussian noise.

The transmit symbols are still in the receive matrix. We eliminate these by element-wise division, yielding

$$(\mathbf{F})_{k,l} = \sum_{h=0}^{H-1} b_h e^{j2\pi l T_O f_{D,h}} e^{-j2\pi k \tau_h \Delta f} e^{j\varphi_h} + (\mathbf{Z})_{k,l}. \quad (4)$$

Thus, from the incoming samples, we can very simply calculate a matrix  $\mathbf{F}$  which contains complex sinusoids on its columns and rows. The radar problem is therefore transformed into a detection and identification of sinusoids.

To tackle this problem, we have proposed several approaches, such as the periodogram [2], [5] and parametric methods [7]. For this work, the periodogram-based technique is used.

The periodogram is a good, in some cases optimal approach for the identification of sinusoids in time-discrete, one-dimensional signals [8]. Here, we extend it to two dimensions, yielding

$$\text{Per}_{\mathbf{F}}(n, m) = \frac{1}{NM} \left| \sum_{k=0}^{N_{\text{Per}}-1} \left( \sum_{l=0}^{M_{\text{Per}}-1} (\mathbf{F})_{k,l} (\mathbf{W})_{k,l} e^{-j2\pi \frac{lm}{M_{\text{Per}}}} \right) e^{j2\pi \frac{kn}{N_{\text{Per}}}} \right|^2. \quad (5)$$

The result is a discrete periodogram with dimensions  $N_{\text{Per}} \times M_{\text{Per}}$ , which are usually chosen as integer multiples of  $N$  and  $M$ , respectively. The first step is an element-wise multiplication with the matrix  $\mathbf{W}$ , a window matrix, which is created by the dyadic product

$$\mathbf{W} = \frac{1}{\|\mathbf{w}_d\|^2 \|\mathbf{w}_v\|^2} \mathbf{w}_r^T \otimes \mathbf{w}_v, \quad \mathbf{w}_r \in \mathbb{R}^{1 \times N}, \quad \mathbf{w}_v \in \mathbb{R}^{1 \times M}, \quad (6)$$

where  $\mathbf{w}_d$  and  $\mathbf{w}_v$  are one-dimensional windows, such as Dolph-Chebyshev windows. The normalization factor fixes the matrix to unit Frobenius norm, allowing us to switch window types without change the total energy of the periodogram.

By using FFTs and IFFTs to calculate the periodogram, this method can be implemented very efficiently. Further optimization can be achieved by preselecting a part of the periodogram which is most likely to contain relevant information, thereby cropping the periodogram to a smaller size than  $N_{\text{Per}} \times M_{\text{Per}}$ .

Fig. 1 shows a schematic of such a radar and communication system. The signal processing chain has been developed and tested in Matlab, it is currently being ported to GNU Radio to eliminate the need for the Matlab runtime and increase performance.

Detecting and identifying targets corresponds to the detection of peaks in the periodogram. If a peak is found at indices  $(\hat{n}, \hat{m})$ , this corresponds to an estimated target distance of

$$\hat{d} = \frac{\hat{n} c_0}{2\Delta f N_{\text{Per}}}, \quad (7)$$

and a relative velocity of

$$\hat{v} = \frac{\hat{m} c_0}{2f_C T_O M_{\text{Per}}}. \quad (8)$$

The range resolution of an OFDM radar system is given by its bandwidth whereas its Doppler resolution is determined by the duration of a frame. However, since the matrix  $\mathbf{F}$  is discrete in nature, there are maximum unambiguous ranges and relative velocities,

$$d_{\text{unamb}} = \frac{c_0}{2\Delta f}, \quad (9)$$

$$v_{\text{unamb}} = \frac{c_0}{2f_C \cdot T_O}. \quad (10)$$

Objects at distances  $d$  and  $d + d_{\text{unamb}}$  can not be distinguished. If these values are chosen large enough, this is not a problem since further objects are less likely to reflect enough energy to appear above the noise floor in any case. However, for large sub-carrier distances it is not unlikely that large objects (e.g. buildings) far away may eclipse a smaller object close by.

#### A. IEEE 802.11a signals

Our combination of (unmodified) USRPs and XCVR2450 daughterboards allows only bandwidths below 36 MHz due to the MAX2829 transceiver IC used on said daughterboard. Since bandwidth fundamentally affects the range resolution, this brings some disadvantages and does not allow to reproduce the exact measurements performed in [3]. However, it is enough to use OFDM signals parametrized according to

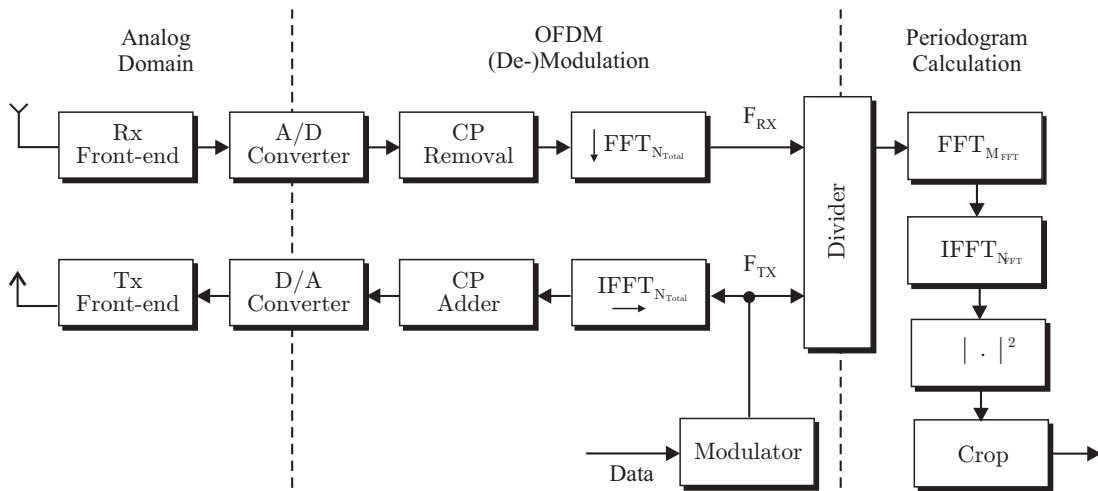
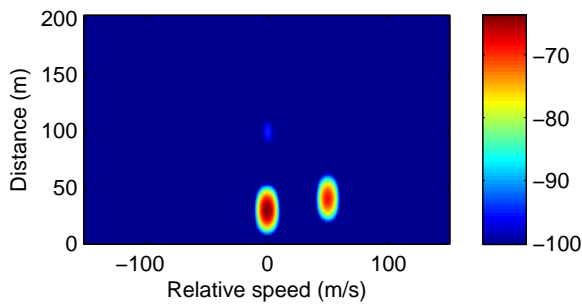
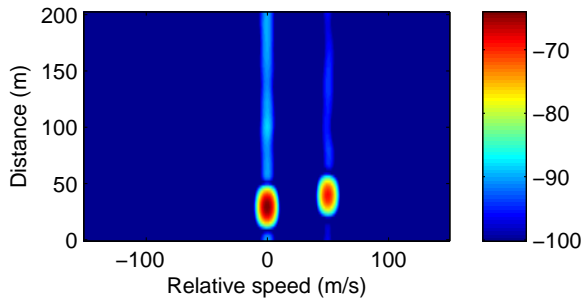


Fig. 1: Schematic of an OFDM radar system



(a) Continuous carrier allocation.



(b) Empty DC carrier. The third target is only barely visible among the spur floor from the closest target.

Fig. 2: Simulated periodograms for three targets

the IEEE 802.11a/p standards [9] which operate at channel bandwidths of 5, 10 or 20 MHz.

OFDM signals according to this standard use  $N = 53$  carriers, including the DC carrier which is left empty to avoid spurs typically induced by direct conversion architectures. The number of OFDM symbols is not specified in the standard, but determined by the number of bits transmitted per packet.

At the 20 MHz channel spacing, the sub-carrier distance is  $\Delta f = 20 \text{ MHz}/64 = 312.5 \text{ kHz}$ . This corresponds to an unambiguous range of  $d_{\text{unamb}} = 480 \text{ m}$ . However, the periodogram is

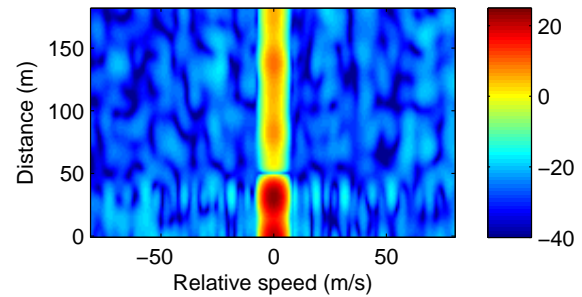


Fig. 3: Spur floor measured with the USRP setup.

only an effective tool if *all* sub-carriers are allocated. Since the DC carrier is left at zero value, the periodogram is calculated with an “incomplete” matrix  $\mathbf{F}$ , which results in spurs. Fig. 2 illustrates how these affect the periodogram; they effectively reduce the dynamic range at a given Doppler value at which at least one target was detected and can thus overshadow targets reflecting less energy. For a more detailed explanation on this phenomenon, we refer to [10].

An easy solution to this problem is to skip every second carrier (including the one at DC). This way, the entire bandwidth is sampled at regular intervals, thus avoiding the aforementioned spurs. Skipping half of the sub-carriers comes with two side effects: First, half of the energy used for transmission is not used for the radar imaging. However, since both our test setup as well as typical wi-fi base stations have a much larger power output than typical vehicular radar systems, this is not a major drawback. Far worse is the reduction of the unambiguous range. Since  $\Delta f$  is effectively doubled,  $d_{\text{unamb}}$  is reduced to 240 m.

Avoiding both DC-carrier related spurs and unambiguous range reduction can only be achieved by using non-standard OFDM signals, e.g. by doubling the number of sub-carriers and thereby reducing the sub-carrier distance before skipping

every second carrier.

The possibility of avoiding DC-carrier related spur floors is another advantage of our OFDM radar approach over other approaches, such as in [11], which use correlation between transmit and receive signals in the time domain.

### B. Use case: Dual Vehicle-to-infrastructure and radar system

In the same context with car-to-car communications, *car-to-infrastructure* communications has also been proposed as means to connect vehicles to the internet. Base stations located at the road side might use the 802.11a/p to connect with vehicles. Using OFDM radar, such a base station can be easily upgraded with a radar component.

Such systems could be used to gather traffic statistics, including vehicles' velocities, or even in the context of traffic enforcement.

## III. MEASUREMENT SETUP

Our measurement setup consists of two USRP N210, each equipped with XCVR2450 daughterboards to allow transmission and reception in the 5 GHz range. The USRPs are synchronized using a MIMO connector cable which also allows to control both devices using a single Ethernet connection.

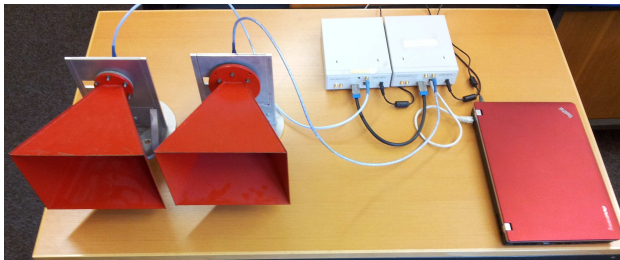


Fig. 4: The measurement setup, showing both USRPs, the controlling laptop and the horn antennas

We used different antennas depending on the measurement setup. For stationary measurements, we used horn antennas with a very high gain of 18.5 dBi (see Fig. 4), which allows for very controlled experiments and reduces direct coupling. For mobile measurements, the USRPs were connected to patch antennas installed into the rear bumper of a VW Sharan.

In their current version, an unmodified USRP can receive and transmit at sampling rates up to 50 Msps. As mentioned before, the available bandwidth is therefore limited by the XCVR2450 daughterboards which allow for a maximum receiver bandwidth of 36 MHz [12].

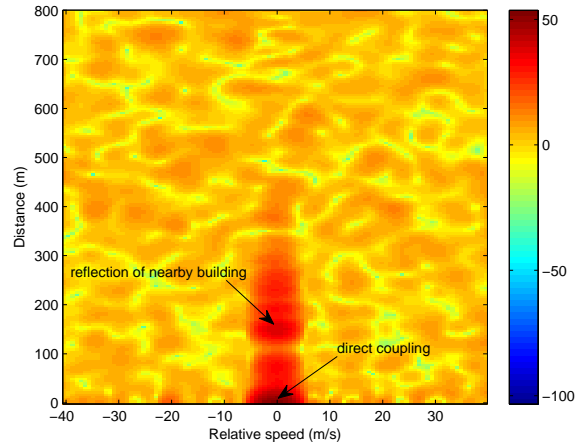
### A. Software setup

The signal processing is performed in Matlab, access to the USRPs is done using a separate, custom-built executable which uses the Universal Hardware Driver (UHD). With this setup, we can switch from simulations to measurements from within Matlab, allowing for faster debugging.

The USRP-controlling software takes a complete frame from Matlab, then loads it into the SRAM of the transmitting



(a) Measurement setup on the rooftop



(b) Periodogram

Fig. 5: Rooftop measurements at 10 MHz bandwidth

USRP. At 16 bit resolution, this limits frames to a total of 262144 samples, but it clears the Ethernet connection for the received signal, thus avoiding overflows. This way, we can currently produce radar images at an update rate of 10 Hz.

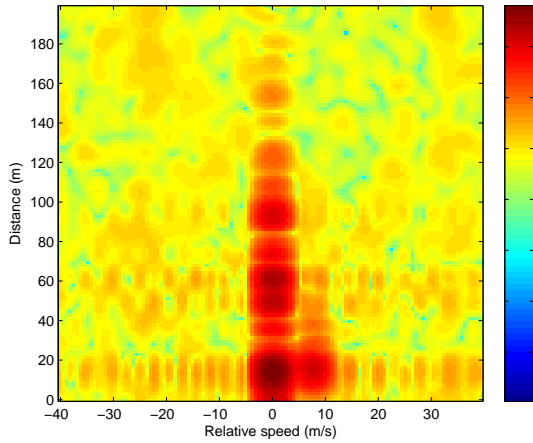
## IV. MEASUREMENT RESULTS

Initial measurements were performed from a rooftop, above the usual clutter such as trees and parked vehicles (Fig. 5a). With only a few buildings as reflecting objects, this was an ideal scenario for testing and calibration purposes. Fig. 5b shows a periodogram of measurement using a relatively small bandwidth of 10 MHz. It immediately highlights a major disadvantage of the OFDM radar system: Direct coupling is apparent as a target with zero range and Doppler. Because the gain stage must be configured such that the direct coupling does not saturate the ADC, this limits the available dynamic range. Coupling is unavoidable as the USRPs need to be connected directly using the MIMO cable; the amount of coupling caused by the horn antennas is in fact negligible.

When running measurements with no antennas attached, we can determine the ratio of the direct coupling to the noise floor to be approx. 55 dB at a sampling rate of 20 MHz.



(a) Measurement setup



(b) Measurement result

Fig. 6: Stationary setup with a vehicle approaching at a speed of approx. 8 m/s

The stationary measurements were also performed on the ground (Fig. 6a). Despite all the clutter, it was possible to detect moving objects (e.g. a car, Fig. 6b).

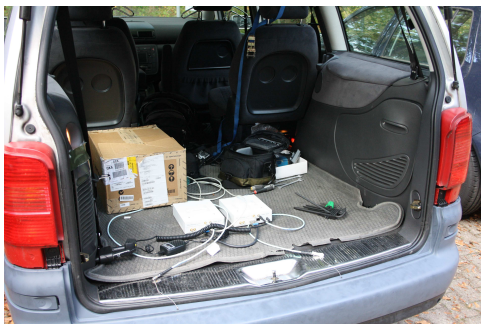


Fig. 7: Setup for motorway measurements

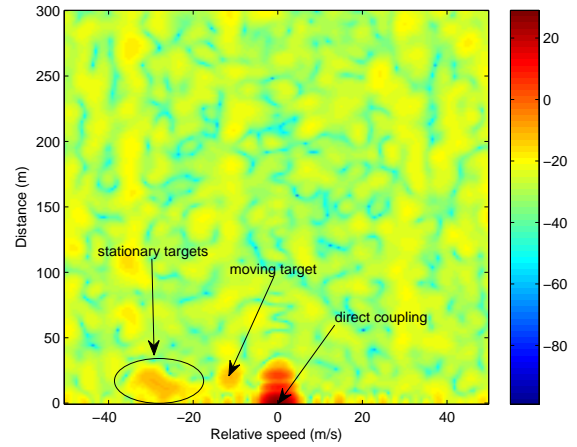


Fig. 8: Measurement on motorway with mobile measurement setup and stationary/moving targets

Measurements from a moving vehicle were also performed (Fig. 7). Unfortunately, the direct coupling induced by the patch antennas, installed in a slightly curved rear bumper only approx. half a metre above the ground, was much stronger and thus the available dynamic range was a lot smaller. However, the periodogram in Fig. 8 clearly shows the following vehicle at a slower velocity as well as stationary objects at a relative velocity of approx. 30 m/s.

## V. CONCLUSION

The USRP-based setup is an improvement over the previous measurement systems in terms of power usage, size, weight, cost and flexibility. It is an easy-to-use system which can be installed into vehicles or used in a stationary setup. We were able to run measurements and show that they concur with simulations.

## ACKNOWLEDGEMENTS

The authors would like to thank Lars Reichardt and Christian Sturm from the Institut für Hochfrequenztechnik und Elektronik (IHE) for supporting us with the mobile measurements.

## REFERENCES

- [1] C. Sturm, E. Pancera, T. Zwick, and W. Wiesbeck, "A Novel Approach to OFDM Radar Processing," *Radar Conference, IEEE*, May 2009.
- [2] C. Sturm, T. Zwick, and W. Wiesbeck, "An OFDM System Concept for Joint Radar and Communications Operations," *Vehicular Technology Conference, 2009. 69th IEEE*, April 2009.
- [3] C. Sturm, M. Braun, T. Zwick, and W. Wiesbeck, "Performance Verification of Symbol-Based OFDM Radar Processing," *Radar Conference, IEEE International*, 2010.
- [4] M. Fuhr, M. Braun, C. Sturm, L. Reichardt, and F. K. Jondral, "An SDR-based Experimental Setup for OFDM-based Radar," *Proceedings of the 7th Karlsruhe Workshop on Software Radio Karlsruhe*, March 2012.
- [5] M. Braun, C. Sturm, and F. K. Jondral, "Maximum Likelihood Speed and Distance Estimation for OFDM Radar," *Radar Conference, IEEE International*, 2010.
- [6] M. I. E. Skolnik, Ed., *Radar handbook*, 2nd ed. Norwich, NY: Knovel, 2003.
- [7] M. Braun, C. Sturm, and F. K. Jondral, "On the Single-Target Accuracy of OFDM Radar Algorithms," *22nd IEEE Symposium on Personal Indoor and Mobile Radio Communications*, 2011.
- [8] S. M. Kay, *Modern Spectral Estimation*. Prentice Hall, 1988.
- [9] *IEEE 802.11 Standard, Part 11*, 2005.
- [10] M. Braun, M. Fuhr, and F. K. Jondral, "Spectral Estimation-based OFDM Radar Algorithms for IEEE 802.11a Signals," *Vehicular Technology Conference, 2012. 76th IEEE*, September 2012.
- [11] P. Falcone, F. Colone, C. Bongioanni, and P. Lombardo, "Experimental results for OFDM WiFi-based passive bistatic radar," in *Radar Conference, 2010 IEEE*, May 2010.
- [12] *Maxim MAX2829 datasheet*. [Online]. Available: [www.maxim-ic.com](http://www.maxim-ic.com)